 doi:10.20944/preprints202205.0039.v1

Article

Structural and optical characterization of mechanochemically synthesized $CuSbS_2$ compounds

Luís Esperto[1], Isabel Figueira[1], João Mascarenhas[1], Teresa Pena Silva[2], José Brito Correia[1], Filipe Neves[1]*

[1] LNEG, Laboratório Nacional de Energia e Geologia, Estrada do Paço do Lumiar, 22, 1649-038 Lisboa, Portugal; luis.esperto@lneg.pt (L.E.); isabel.figueira@lneg.pt (I.F.); joao.mascarenhas@lneg.pt (J.M.); brito.correia@lneg.pt (J.B.C); filipe.neves@lneg.pt (F.N.)

[2] LNEG, Laboratório Nacional de Energia e Geologia, Estrada da Portela, Bairro do Zambujal – Alfragide, Apartado 7586, 2610-999 Amadora, Portugal; teresa.pena@lneg.pt (T.P.S.)

* Correspondence: filipe.neves@lneg.pt

Abstract: One of the areas of research on materials for thin-film solar cells focuses on replacing In and Ga with more earth-abundant elements. In that respect, chalcostibite ($CuSbS_2$) is being considered as a promising environmentally friendly and cost-effective photovoltaic absorber material. In the present work, single $CuSbS_2$ phase have been synthesized directly by a short duration (2 h) mechanochemical synthesis step starting from mixtures of elemental powders. X-ray diffraction analysis of the synthesized $CuSbS_2$ powders revealed a good agreement with the orthorhombic chalcostibite phase, space group Pnma, and a crystallite size of 26 nm. Particle size characterization revealed a multimodal distribution with a median diameter ranging from of 2.93 μm to 3.10 μm. The thermal stability of the synthesized $CuSbS_2$ powders was evaluated by differential thermal analysis. No phase change was observed by heat treating the mechanochemically synthesized powders at 350 °C for 24 h. By UV-VIS-NIR spectroscopy the optical bandgap was determined to be 1.41 eV, suggesting that the mechanochemically synthesized $CuSbS_2$ can be considered suitable to be used as absorber materials. Overall, the results show that the mechanochemical process is a viable route for the synthesis of materials for photovoltaic applications.

Keywords: powder technology; mechanochemical synthesis; absorber materials; chalcostibite

1. Introduction

The photovoltaic (PV) market is dominated by the c-Si technology, with thin-film (TF) market share technology representing about 5% of today's global annual market [1]. Within the TF technology, CdTe and $Cu(In,Ga)Se_2$ (CI(G)S) are already well established [1]. Another emerging pre-commercial TF technology is hybrid organic-inorganic perovskite $CH_3NH_3PbI_3$ [2]. However, to satisfy the expected world´s energy demand for the next decades, in the TW scale, these technologies present some limitations [2]: the capital intensity of Si may be difficult to reduce, environmental friendliness of Cd and Pb are questionable, and earth-abundance of In, Ga, and Te are under debate.

In recent years, the research is being focused on the replacement of In and Ga with more earth-abundant elements, such as Zn and Sn, resulting in 12.6% efficient $Cu_2ZnSn(S,Se)_4$ (CZTS) thin-film solar cell (TFSC) device [2,3]. However, further improvements in the CZTS are being hampered by compositional heterogeneities, complex defect chemistry and strong tendency for disorder [2]. These limitations are leading to the research of absorber materials based on less complex chalcogenides compounds, such as the Cu–Sb–S (CAS) based materials [2,4].

In the CAS system, the most promising phase known to have good prospect as absorber material for new single-junction or tandem TFSCs is $CuSbS_2$ (chalcostibite) because of its high optical absorption coefficient (over 10^5 cm^{-1}), p-type electrical conductivity, tunable optical bandgap (1.4-1.5 eV), low fabrication temperatures and a

 doi:10.20944/preprints202205.0039.v1

high value of spectroscopic limited maximum efficiency of 22.9% [4,5]. However, up to now the TFSCs efficiencies with $CuSbS_2$ absorbers remain close to 3% [6].

A variety of physical and chemical methods can be used for the synthesis of metal chalcogenides absorber materials, in which the use of advanced powder technologies is included [7–10]. Within them, the use mechanochemical synthesis (MCS) process, a solid-state synthesis route using high-energy ball mills, is being considered as a faster, scalable and environmentally friendly technology than the conventional processing routes for producing chalcogenides compounds [11–14].

The present work describes experimental studies related with the direct synthesis of $CuSbS_2$ by a short duration MCS step starting from mixtures of elemental powders. The observed strong thermal stability of the structure and the determined optical bandgap of 1.41 eV allow us to infer the suitability of the MCS process for the production of PV materials and the potentialities of the synthesized materials as absorbers for TFSCs.

2. Materials and Methods

The $CuSbS_2$ powders were synthesized by MCS performed on a Retsch high-energy planetary ball mill PM400. Mixtures of the elemental copper (Cu; Alfa Aesar, 99.9%, 10 μm), antimony (Sb; Sigma-Aldrich, 99.5%, < 149 μm) and sulfur (S; Alfa Aesar, 99.999%, random sizes) powders, in the ratio of 1:1:2, were filled into 250 mL stainless steel jars together with 26 balls with a diameter of 15 mm and without any additional fluid medium. These experiments were performed at a rotational speed of 340 rpm for a total milling duration of 2 h. Before starting the MCS, the jars were evacuated and back-filled with Argon. A small fraction of the MCS powders was heat treated in vacuum (10^{-2} mbar) at 350 °C for 24 h using a conventional tube furnace.

Powder X-ray diffraction data was collected using a D8 Advance Bruker AXS diffractometer with Cu Kα radiation. The XRD data treatment was performed by using DIFFRAC.EVA v5 software (Bruker AXS) [15], for phase identification, and DIFFRAC.TOPAS v6 software (Bruker AXS) [16], for a full pattern Rietveld refinement [17]. As a measure for the goodness of the refinements the weighted profile R factor, R_{wp}, has been used. Morphology and chemical elemental mapping of the powder particles was obtained, respectively, by scanning electron microscopy (SEM) and energy dispersive X-ray spectroscopy (EDS) using a Philips XL30 field emission SEM fitted with a Thermo Scientific™ UltraDry EDS detector. Particle size distribution of the produced $CuSbS_2$ powders was determined with a CILAS 1064 laser granulometer. Differential thermal analysis (DTA) was performed on a Setaram TG-DTA 92-16 thermobalance to evaluate the thermal stability of the synthesized powders from room temperature up to 600 °C. The DTA experiments were carried out in specimens with masses of around 50 mg, with heating and cooling rates of 7 °C min^{-1} and under a high purity Argon gas flow. Diffuse reflectance spectra were collected using a PerkinElmer Lambda 950 UV/Vis/NIR Spectrophotometer, with InGaAs integrating sphere, in the spectral range of 350–1250 nm for bandgap energy assessment.

3. Results and Discussion

Figure 1 shows the XRD pattern of the mechanochemically synthesized $CuSbS_2$ powders. All the main reflections from the XRD pattern can be assigned to the $CuSbS_2$ chalcostibite orthorhombic structure with the space group Pnma (62) (COD 9003580 [18]). Additionally, no secondary phases were detected while the observable broadening of the Bragg peaks is mainly a consequence of the MCS process, which causes low crystallite size [19]. This result reflects the successful and fast conversion of the pristine elements into the chalcostibite phase with the experimental conditions used in the MCS. The reaction pathway leading to the direct synthesis of the chalcostibite $CuSbS_2$ compound during the MCS process can be roughly assumed to follow the same path reported for other ternary chalcogenides [20,21]: 1) at the early stage of the MSC, the reaction between Cu and S occurs resulting in the formation of Cu-S binary compounds; 2) with the continuation of

Preprints (www.preprints.org) | NOT PEER-REVIEWED | Posted: 5 May 2022 doi:10.20944/preprints202205.0039.v1

the MCS, Sb starts to be involved in the reaction with the Cu-S binary compounds giving rise to the formation of the ternary chalcostibite $CuSbS_2$ compound.

Typical Rietveld analysis outputs for the 2 h MCS $CuSbS_2$ powders are presented in Figure 2. The orthorhombic structure with the space group Pnma (62) mentioned above was used as structural model in the refinement. As it can be seen, there is a good match between the calculated XRD pattern and the observed XRD pattern. This is corroborated by the values obtained for the R factors (R_{exp} = 2.56% and R_{wp} = 3.80%) which ensure the good level of the refinement. The obtained Rietveld refined structural lattice parameters are a = 6.0222(2) Å, b = 3.80317(16) Å and c = 14.5043(6) Å. These values are in good with the reference values for the chalcostibite orthorhombic structure from the COD 9003580 file (a = 6.018 Å, b = 3.7958 Å and c = 14.495 Å). Moreover, the crystallite size for the mechanochemically synthesized $CuSbS_2$ powders was calculated to be 26.5(4) nm.

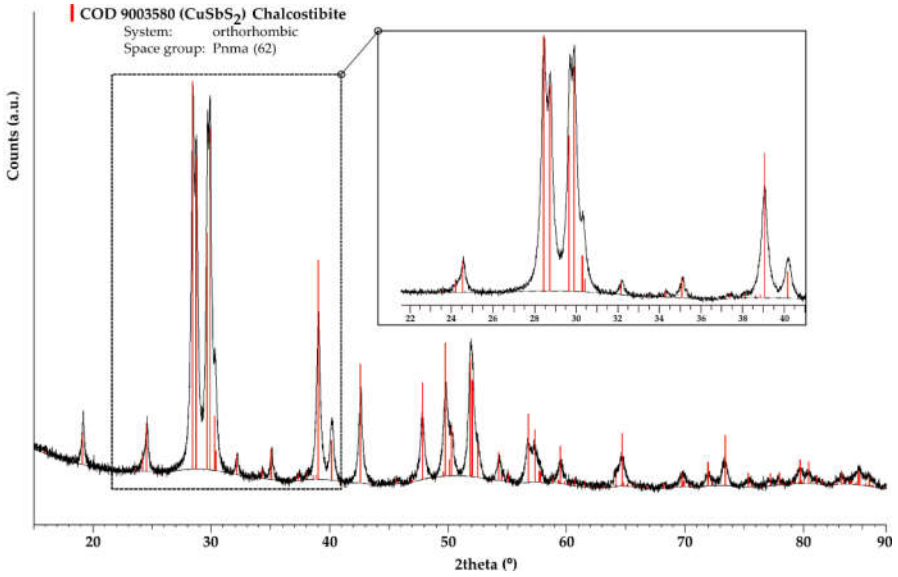

Figure 1. XRD pattern of $CuSbS_2$ powders produced directly by mechanochemical synthesis for 2 h.

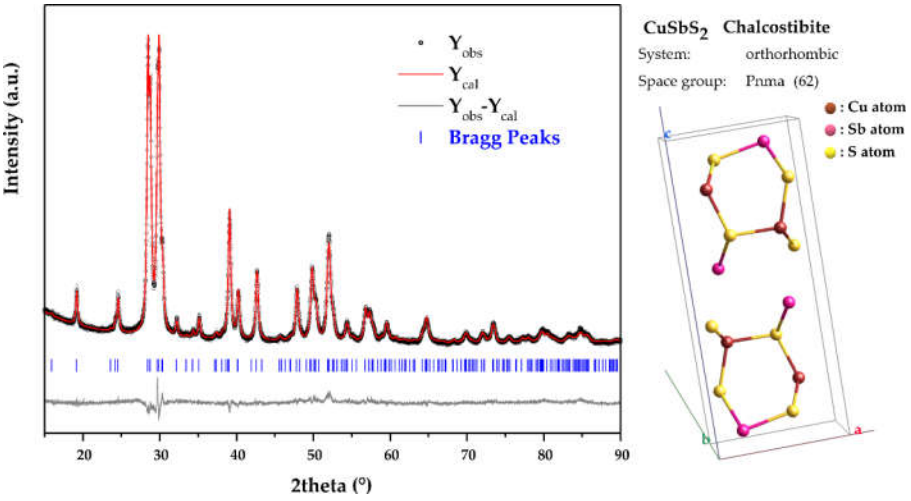

Figure 2. Rietveld refinement of the XRD pattern of $CuSbS_2$ powders directly produced by mechanochemical synthesis.

The morphology of the mechanochemically synthesized $CuSbS_2$ powders is shown in Figure 3(a). Based on SEM observations, the powder particles exhibit a quite irregular morphology, generically presenting three types of fractions: one at the submicrometric

Preprints (www.preprints.org) | NOT PEER-REVIEWED | Posted: 5 May 2022 doi:10.20944/preprints202205.0039.v1

scale and the other two of the order of a few μm to tens of μm. In addition, it was seen that the submicron fraction tends to aggregate in micron-sized agglomerates. These observations were corroborated by the values of the characteristic dimensions of the particles (D10, D50 and D90) and by the granulometric distribution evaluated by laser diffractometry. As seen in Figure 3(b), the frequency distribution curve (q3, histogram) revealed a multimodal distribution with three maxima. Moreover, the values obtained for D10, D50 and D90 means that 10% of the $CuSbS_2$ powder particles are smaller than 0.52 μm, 50% are smaller than 3.02 μm, and 90% are smaller than 14.19 μm.

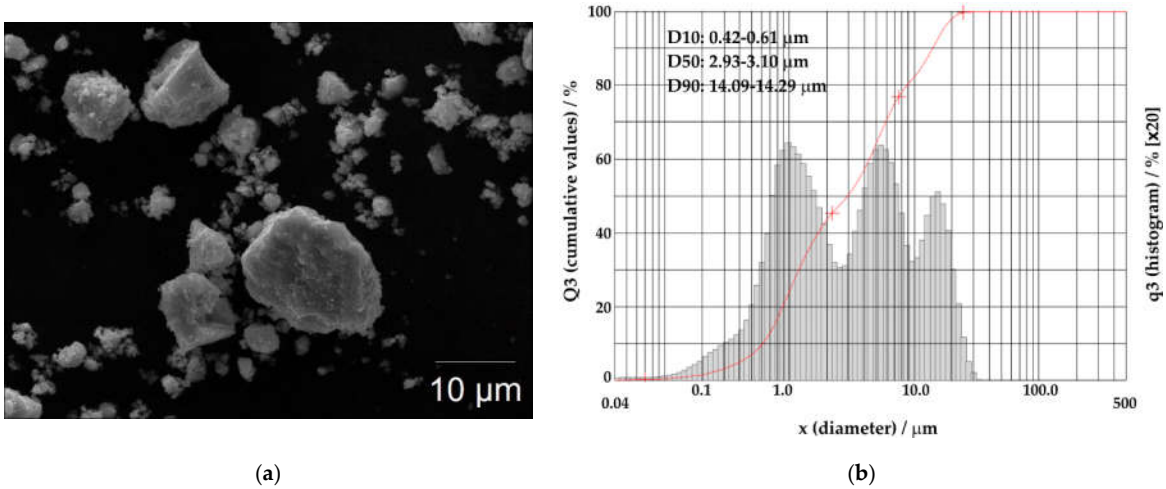

(**a**) (**b**)

Figure 3. (**a**) SEM image and (**b**) cumulative particle size distribution and histogram of particle size distribution of the $CuSbS_2$ powders directly produced by mechanochemical synthesis.

EDS maps of the individual elements Cu, Sb and S allowed to address the degree of homogeneity of those elements within the produced $CuSbS_2$ powder particles. As show in Figure 4, all the elements are evenly distributed throughout the analyzed powder particles. Considering the starting elemental powder mixture, the uniform and homogeneous spatial distribution of Cu, Sb and S after the MCS process is extremely relevant.

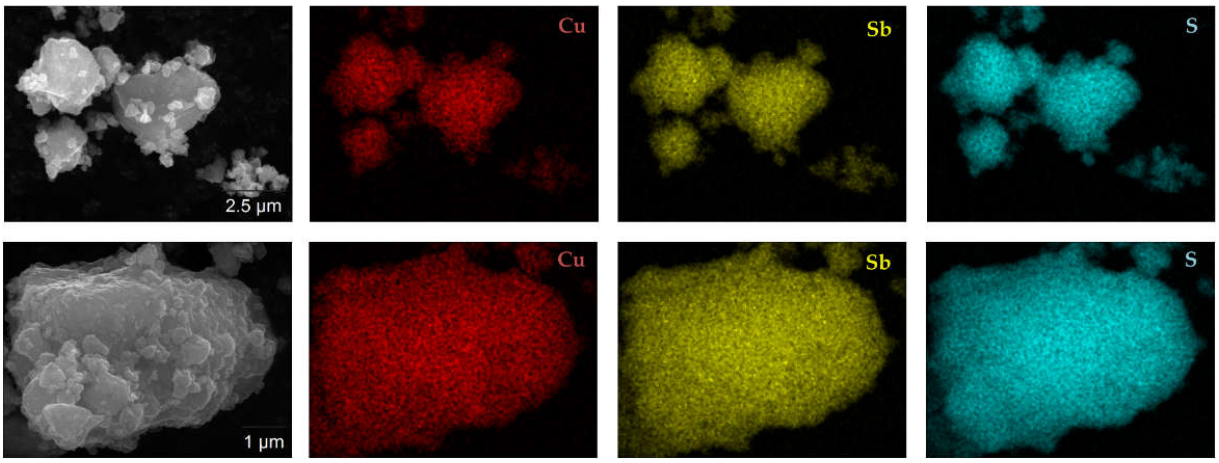

Figure 4. EDS elemental mapping for the $CuSbS_2$ powder particles directly produced by mechanochemical synthesis.

The DTA heating curve of the mechanochemically synthesized $CuSbS_2$ powders is shown in Figure 5. For temperatures above 400 °C it reveals two small endothermic peaks that are associated to the onset of the thermal decomposition of the chalcostibite $CuSbS_2$ phase. According to the literature, the products of this thermal decomposition are

Preprints (www.preprints.org) | NOT PEER-REVIEWED | Posted: 5 May 2022 doi:10.20944/preprints202205.0039.v1

$Cu_{12}Sb_4S_{13}$, Sb_2S_3, and Sb_4 [4,22]. The endothermic peak at 551 °C corresponds to the melting [4,22].

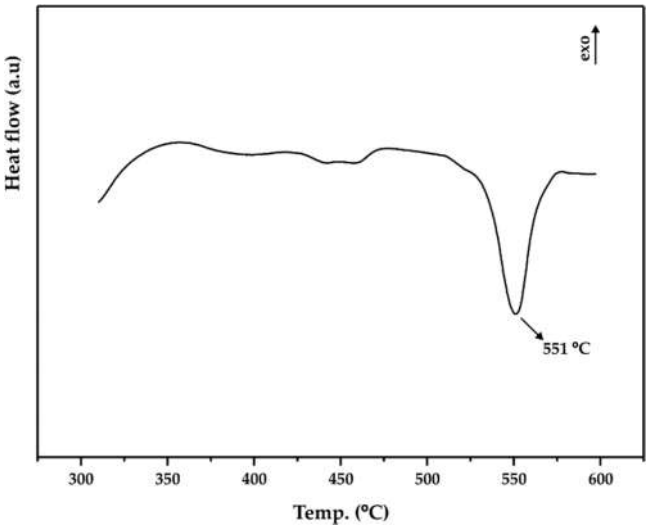

Figure 5. DTA heating curve of mechanochemically synthesized $CuSbS_2$ powders.

The thermal structural stability of the produced chalcostibite $CuSbS_2$ phase was also addressed by XRD of the heat treated mechanochemically synthesized $CuSbS_2$ powders at 350 °C for 24 h in vacuum. It should be mentioned that the temperature chosen for this heat treatment was intentionally selected below the onset of the thermal decomposition of the chalcostibite $CuSbS_2$ phase. As illustrated in Figure 6, all the main reflections from the obtained XRD pattern were again assigned to the orthorhombic structure with the space group Pnma (62). However, when compared to Figure 1, the observed Bragg peaks are now sharper and better defined. This can be attributed to the increase of the crystallite size and reduction of internal strains.

Figure 7 shows the Rietveld analysis outputs for the heat treated $CuSbS_2$ powders. The values obtained for the R factors (R_{exp} = 2.29% and R_{wp} = 5.20%) confirm the good level of the refinement with the orthorhombic structure with the space group Pnma (62). The obtained Rietveld refined structural lattice parameters are a = 6.02061(4) Å, b = 3.80171(2) Å and c = 14.50051(10) Å (Table 1). As expected, these results put in evidence the recovery of the crystal structure due to the heat treatment and, as a consequence, the lattice parameters are closer to the standard values for the chalcostibite orthorhombic structure from the COD 9003580 file (Table 1). Moreover, this was also supported by the crystallite size determined for the heat treated $CuSbS_2$ powders, which was calculated to be 141(5) nm and, consequently, greater than the crystallite size value shown above (26.5(4) nm) for the mechanochemically synthesized powders.

Table 1. Results of the Rietveld refinement for the lattice parameters of the mechanochemically synthesized $CuSbS_2$ powders and of the heat treated $CuSbS_2$ powders. For comparison purposes, the standard values from the COD 9003580 file are also shown.

Lattice parameter (Å)	MCS	Heat treated	COD 9003580 file
a	6.0222(2)	6.02061(4)	6.018
b	3.80317(16)	3.80171(2)	3.7958
c	14.5043(6)	14.50051(10)	14.495

Preprints (www.preprints.org) | NOT PEER-REVIEWED | Posted: 5 May 2022 doi:10.20944/preprints202205.0039.v1

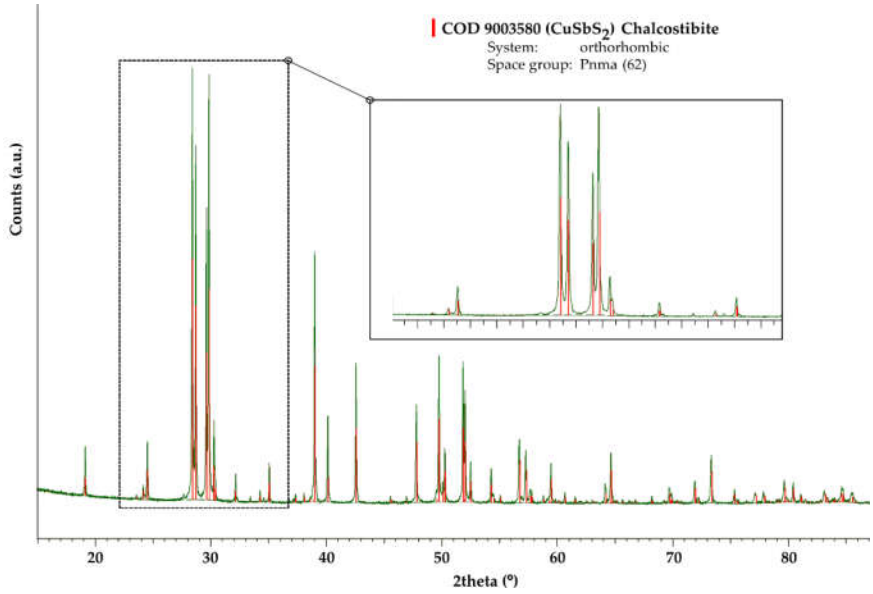

Figure 6. XRD pattern of mechanochemically synthesized $CuSbS_2$ powders heat treated at 350 ºC/ 24 h.

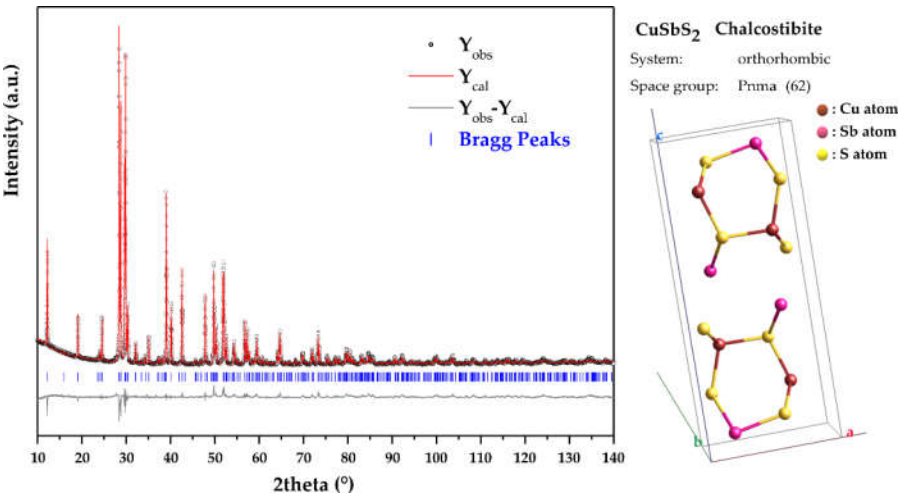

Figure 7. Rietveld refinement of the XRD pattern of mechanochemically synthesized $CuSbS_2$ powders heat treated at 350 °C/ 24 h.

As shown in Figure 8, the optical bandgap (*Eg*) estimation was performed by extrapolating the linear region of the Tauc plot to the horizontal axis and considering the intersecting point [23]. This has led to an *Eg* of 1.41 eV for the mechanochemically synthesized chalcostibite material, which is consistent with the theoretical and experimental values reported in the literature [4,24]. Consequently, the produced chalcostibite materials possess the expected optical characteristics. Considering that the optimal *Eg* should be in the range of 1.0-1.5 eV, the obtained result is very promising and can facilitate their potential application as an alternative absorber material for thin film solar cells. Thus, the ability to form thin films from the mechanochemically synthesized $CuSbS_2$ powder, also using non-vacuum processes, is important for solar cell fabrication and is being the subject of current studies.

 doi:10.20944/preprints202205.0039.v1

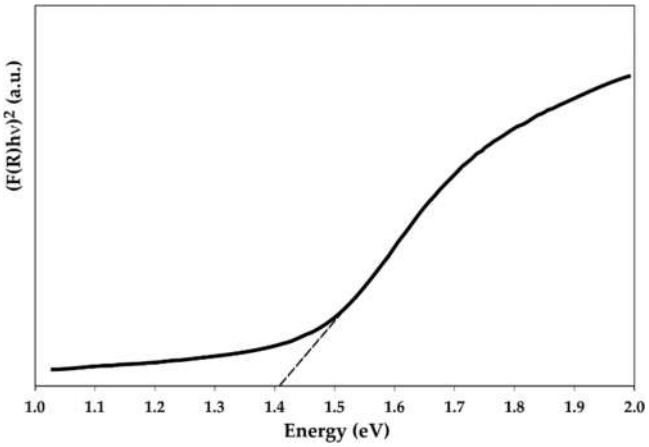

Figure 8. Tauc plot for the $CuSbS_2$ compound directly produced by mechanochemical synthesis.

4. Conclusions

Powders of $CuSbS_2$, having orthorhombic structure with the space group Pnma (62), were synthesized directly through a short 2 h duration mechanochemical step. The absence of any phase transformation with the heat treatment at 350 °C for 24 h, demonstrated the strong structural stability of the produced phase. The bandgap energy of the $CuSbS_2$ powders was estimated by extrapolation to be of 1.41 eV, in good agreement to the values reported in the literature. The mechanochemically synthesized $CuSbS_2$ compounds can then be considered suitable to be used as absorber materials for thin-film solar cells. Furthermore, the mechanochemical synthesis process proved to be a viable and promising route for the preparation of materials for photovoltaic applications.

Author Contributions: Conceptualization, J.B.C and F.N.; investigation, L.E., I.F., J.M., and T.P.S.; writing—original draft preparation, J.B.C. and F.N.; writing—review and editing, L.E., I.F., J.M., T.P.S., J.B.C. and F.N.; project administration, F.N.; funding acquisition, F.N. All authors have read and agreed to the published version of the manuscript.

Funding: This work is funded by national funds through the FCT – Fundação para a Ciência e a Tecnologia, I.P., under the project PTDC/EAM-PEC/29905/2017 (LocalEnergy project, http://localenergy.lneg.pt).

Institutional Review Board Statement: Not applicable.

Informed Consent Statement: Not applicable.

Data Availability Statement: Data are contained within the article.

Acknowledgments: The "Direção Geral de Energia e Geologia" participates as an "External Advisor" in LocalEnergy project.

Conflicts of Interest: The authors declare no conflict of interest.

References

1. Report, ©Fraunhofer ISE: Photovoltaics *Photovoltaics Report*; 2022;
2. Zakutayev, A. Brief Review of Emerging Photovoltaic Absorbers. *Curr. Opin. Green Sustain. Chem.* **2017**, *4*, 8–15, doi:10.1016/j.cogsc.2017.01.002.
3. Wang, W.; Winkler, M.T.; Gunawan, O.; Gokmen, T.; Todorov, T.K.; Zhu, Y.; Mitzi, D.B. Device Characteristics of CZTSSe Thin-Film Solar Cells with 12.6% Efficiency. *Adv. Energy Mater.* **2014**, *4*, 1–5, doi:10.1002/aenm.201301465.
4. Peccerillo, E.; Durose, K. Copper—Antimony and Copper—Bismuth Chalcogenides—Research Opportunities and Review for Solar Photovoltaics. *MRS Energy Sustain.* **2018**, *5*, doi:10.1557/mre.2018.10.
5. De Souza Lucas, F.W.; Zakutayev, A. Research Update: Emerging Chalcostibite Absorbers for Thin-Film Solar Cells. *APL Mater.* **2018**, *6*, doi:10.1063/1.5027862.

6. Banu, S.; Ahn, S.J.; Ahn, S.K.; Yoon, K.; Cho, A. Fabrication and Characterization of Cost-Efficient CuSbS2 Thin Film Solar Cells Using Hybrid Inks. *Sol. Energy Mater. Sol. Cells* **2016**, *151*, 14–23, doi:10.1016/j.solmat.2016.02.013.
7. Lokhande, A.C.; Chalapathy, R.B.V.; He, M.; Jo, E.; Gang, M.; Pawar, S.A.; Lokhande, C.D.; Kim, J.H. Development of Cu2SnS3 (CTS) Thin Film Solar Cells by Physical Techniques: A Status Review. *Sol. Energy Mater. Sol. Cells* **2016**, *153*, 84–107, doi:10.1016/j.solmat.2016.04.003.
8. Li, C.; Yao, B.; Li, Y.; Xiao, Z.; Ding, Z.; Zhao, H.; Zhang, L.; Zhang, Z. Fabrication, Characterization and Application of Cu2ZnSn(S,Se)4 Absorber Layer via a Hybrid Ink Containing Ball Milled Powders. *J. Alloys Compd.* **2015**, *643*, 152–158, doi:10.1016/j.jallcom.2015.04.140.
9. Timmo, K.; Kauk-Kuusik, M.; Pilvet, M.; Raadik, T.; Altosaar, M.; Danilson, M.; Grossberg, M.; Raudoja, J.; Ernits, K. Influence of Order-Disorder in Cu2ZnSnS4 Powders on the Performance of Monograin Layer Solar Cells. *Thin Solid Films* **2017**, *633*, 122–126, doi:10.1016/j.tsf.2016.10.017.
10. Neves, F.; Correia, J.B.; Hanada, K.; Santos, L.F.; Gunder, R.; Schorr, S. Structural Characterization of Cu2SnS3 and Cu2(Sn,Ge)S3 Compounds. *J. Alloys Compd.* **2016**, *682*, doi:10.1016/j.jallcom.2016.05.005.
11. Dutková, E.; Sayagués, M.J.; Fabián, M.; Kováč, J.; Kováč, J.; Baláž, M.; Stahorský, M. Mechanochemical Synthesis of Ternary Chalcogenide Chalcostibite CuSbS2 and Its Characterization. *J. Mater. Sci. Mater. Electron.* **2021**, *32*, 22898–22909, doi:10.1007/s10854-021-06767-9.
12. Neves, F.; Stark, A.; Schell, N.; Mendes, M.J.; Aguas, H.; Fortunato, E.; Martins, R.; Correia, J.B.; Joyce, A. Investigation of Single Phase Cu2ZnSnxSb1-XS4 Compounds Processed by Mechanochemical Synthesis. *Phys. Rev. Mater.* **2018**, *2*, 075404 (9), doi:10.1103/PhysRevMaterials.2.075404.
13. Baláž, P.; Baláž, M.; Sayagués, M.J.; Eliyas, A.; Kostova, N.G.; Kaňuchová, M.; Dutková, E.; Zorkovská, A. Chalcogenide Quaternary Cu2FeSnS4 Nanocrystals for Solar Cells: Explosive Character of Mechanochemical Synthesis and Environmental Challenge. *Crystals* **2017**, *7*, doi:10.3390/cryst7120367.
14. Takei, K.; Maeda, T.; Wada, T. Crystallographic and Optical Properties of CuSbS2and CuSb(S1 -XSex)2solid Solution. *Thin Solid Films* **2015**, *582*, 263–268, doi:10.1016/j.tsf.2014.11.029.
15. Bruker AXS DIFFRAC.EVA v5, Software for the Analysis of 1D and 2D X-Ray Datasets Including Visualization, Data Reduction, Phase Identification and Quantification, Statistical Evaluation 2019.
16. Bruker AXS DIFFRAC.TOPAS v6, Profile Fitting Based Software for Quantitative Phase Analysis, Microstructure Analysis and Crystal Structure Analysis 2016.
17. Rietveld, H.M. A Profile Refinement Method for Nuclear and Magnetic Structures. *J. Appl. Crystallogr.* **1969**, *2*, 65–71.
18. Grazulis, S.; Chateigner, D.; Downs, R.T.; Yokochi, A.F.T.; Quiros, M.; Lutterotti, L.; Manakova, E.; Butkus, J.; Moeck, P.; Le Bail, A. Crystallography Open Database - an Open-Access Collection of Crystal Structures. *J. Appl. Crystallogr.* **2009**, *42*, 726–729.
19. Baláž, P.; Achimovicová, M.; Baláž, M.; Billik, P.; Zara, C.Z.; Criado, J.M.; Delogu, F.; Dutková, E.; Gaffet, E.; Gotor, F.J.; et al. Hallmarks of Mechanochemistry: From Nanoparticles to Technology. *Chem. Soc. Rev.* **2013**, *42*, 7571–7637, doi:10.1039/c3cs35468g.
20. Li, J.; Tan, Q.; Li, J.F. Synthesis and Property Evaluation of CuFeS2-x as Earth-Abundant and Environmentally-Friendly Thermoelectric Materials. *J. Alloys Compd.* **2013**, *551*, 143–149, doi:10.1016/j.jallcom.2012.09.067.
21. Zhang, D.; Yang, J.; Jiang, Q.; Fu, L.; Xiao, Y.; Luo, Y.; Zhou, Z. Ternary CuSbSe2 Chalcostibite: Facile Synthesis, Electronic-Structure and Thermoelectric Performance Enhancement. *J. Mater. Chem. A* **2016**, *4*, 4188–4193, doi:10.1039/c6ta00039h.
22. Welch, A.W.; Zawadzki, P.P.; Lany, S.; Wolden, C.A.; Zakutayev, A. Self-Regulated Growth and Tunable Properties of CuSbS2 Solar Absorbers. *Sol. Energy Mater. Sol. Cells* **2015**, *132*, 499–506, doi:10.1016/j.solmat.2014.09.041.
23. Viezbicke, B.D.; Patel, S.; Davis, B.E.; Birnie, D.P. Evaluation of the Tauc Method for Optical Absorption Edge Determination: ZnO Thin Films as a Model System. *Phys. Status Solidi Basic Res.* **2015**, *252*, 1700–1710, doi:10.1002/pssb.201552007.

 doi:10.20944/preprints202205.0039.v1

24. De Souza Lucas, F.W.; Zakutayev, A. Research Update: Emerging Chalcostibite Absorbers for Thin-Film Solar Cells. *APL Mater.* **2018**, *6*, doi:10.1063/1.5027862.